Available online at www.sciencedirect.com
SCIENCE DIRECT
Spectrochimica Acta Part A 63 (2006) 905–909
SPECTROCHIMICA ACTA PART A
www.elsevier.com/locate/saa

Use of $^{130}Te_2$ for frequency referencing and active stabilisation of a violet extended cavity diode laser

I.S. Burns *, J. Hult, C.F. Kaminski

Department of Chemical Engineering, University of Cambridge, Pembroke Street, Cambridge CB2 3RA, UK

Received 20 September 2005; received in revised form 28 October 2005; accepted 31 October 2005

Abstract

This paper reports on the use of $^{130}Te_2$ absorption lines in active laser-locking, and in frequency referencing, of the emission of a violet extended cavity diode laser with a wavelength of around 410 nm. We note the existence of closely spaced tellurium absorption lines, suitable for referencing purposes in gas sensing applications, at wavelengths below the lower limit (417 nm) of the spectral region covered by the tellurium atlas [J. Cariou, P. Luc, Atlas du spectre d'Absorption de la Molecule de Tellure, CNRS, Paris, 1980]. The absolute positions of the lines in the acquired spectra were estimated by comparison to a simultaneously acquired fluorescence spectrum of atomic indium, and were identified using calculations based on fundamental spectroscopic data. The laser frequency was stabilised within a range of 40 MHz, which is negligible compared to typical transition widths at atmospheric pressure.

Keywords: Tellurium; Indium; Extended cavity; Tunable diode laser; Absorption spectroscopy; Laser induced fluorescence

1. Introduction

Violet extended cavity diode lasers emitting in the spectral region between 394 nm and 417 nm have recently been used in a number of spectroscopic studies [1–6]. A number of atomic and molecular species exhibit strong electronic transitions in this wavelength region, and are of interest both in industrial sensing and in fundamental spectroscopy applications. It is often useful when performing such spectroscopy, to have a means of calibrating the absolute wavelength scale of the laser scan by an external reference source. In some applications, it is also necessary to lock the frequency of the laser using a feedback control loop to compensate for drifts in the effective length of the extended cavity. This serves to ensure that the spectral overlap between the laser and the transition being probed remains constant.

Previous studies have investigated the use of advanced techniques to lock the wavelength of extended cavity diode lasers with very high precision [7,8]. Such systems are developed for use in fundamental atomic physics experiments that are conducted at low pressure. By contrast, industrial and environmental gas sensing applications are typically performed at atmospheric pressure [9], giving rise to much higher transition widths. Therefore, the upper limit of the laser frequency fluctuations that can be tolerated in such applications is much greater, but it is nonetheless important to avoid any long-term drifts in the laser wavelength. In the present study, we demonstrate a straightforward method for stabilising the emission wavelength of violet ECDLs, which would be suitable for gas diagnostic applications.

Diatomic molecules of species such as tellurium and iodine exhibit a dense spectrum of strong absorption lines resulting from the rotational fine structure of electronic-vibration transitions; this is because their high reduced mass gives rise to a low rotational constant, which leads to close rotational line spacing and causes a large number of rotational energy levels to be significantly populated. For this reason, these species are frequently used for referencing the frequency scale of a laser scan, or for locking the wavelength of a laser source. While the iodine spectrum extends from 500 nm to 675 nm [10], the strong tellurium lines occur in the region 385–523 nm [11]. An atlas tabulating the positions of the strong lines in the spectrum of the tellurium isotope $^{130}Te_2$ is available [12], covering the wavelength region above 417 nm. Absorption lines of Te_2 have been used to reference the frequency scale of spectral scans, in the region covered by the atlas [12], in numerous experimental studies; some examples of this have involved the use of blue dye

* Corresponding author. Tel.: +44 1223 334777; fax: +44 1223 334796.
E-mail addresses: isb23@cam.ac.uk (I.S. Burns), jfh36@cheng.cam.ac.uk (J. Hult), cfk23@cam.ac.uk (C.F. Kaminski).

1386-1425/$ – see front matter © 2005 Elsevier B.V. All rights reserved.
doi:10.1016/j.saa.2005.10.053

lasers [13–15]. Spectroscopy of Te_2 has also been performed with a near-infrared diode laser, which was frequency doubled to 493 nm [16]. The $^{130}Te_2$ molecule has also been used to lock the wavelength of visible lines of Ar^+ lasers [17].

In this paper, we first describe the experimental work, which comprises a spectral scan of the $^{130}Te_2$ lines around 410 nm, followed by the use of one of these lines in active stabilisation of the laser wavelength. The resulting absorption spectrum was compared to data from the literature and to theoretical predictions allowing the strong lines to be identified. The laser-locking resulted in a stabilisation of the wavelength within a range of 40 MHz.

2. Experimental

The experiments were performed using a Littrow-configuration extended cavity diode laser (ECDL) emitting at around 410 nm. The extended cavity concept involves the use of optical feedback from a grating to force the Fabry–Perot diode laser to emit on a single longitudinal mode [18]. The ECDL system used during these experiments has been described in detail previously [19], and is capable of performing mode-hop free tuning over wide bandwidths by synchronous tuning of the electrical signals applied to piezo-electric transducers in the grating mount, and of the diode laser injection current.

In the first part of the experiment, absorption spectra of $^{130}Te_2$ and fluorescence spectra of In were acquired simultaneously; the experimental set-up is shown in Fig. 1. The laser beam was focussed at a point several millimetres above the reaction zone of a laminar Bunsen flame of premixed methane and air, which was slightly fuel-rich. The flame was seeded with indium atoms by passing the air stream through a nebuliser containing an aqueous solution of $InCl_3$. The collection and detection of the atomic fluorescence signal was performed exactly as described previously [9]. The indium fluorescence spectrum was used to calibrate the frequency scale of the simultaneously acquired tellurium absorption spectra. Before passing through the flame, a part of the laser beam was reflected by a glass plate and directed towards a quartz cell containing isotopically pure $^{130}Te_2$ (Opthos Instruments; path length = 10 cm). The cell had been mounted in a ceramic furnace and was held at a constant temperature of around 670 °C throughout the experiment; the temperature was measured by a thermocouple in contact with the exterior of the absorption cell. No buffer gas was present so the total pressure in the cell was equal to the vapour pressure of $^{130}Te_2$, which was estimated to be around 3 Torr. Single-mode tuning of the laser wavelength was performed at scan-rate of 20 Hz over a range of approximately 70 GHz. The intensity of the beam transmitted through the cell was measured by a photodiode. Another reflection of the main laser beam was directed on to a second photodiode as a reference intensity measurement. A third reflection from the laser beam was directed into an air-spaced etalon (FSR = 5.07 GHz; $F = 6$), whose free spectral range was determined from the spacing between the hyperfine components of the indium fluorescence spectrum, described below and shown in Fig. 2. The etalon transmission pattern was later used to linearise the frequency scale of the scans. The signals were digitised using a data acquisition card (National Instruments PCI-6014). Having acquired $^{130}Te_2$ absorption spectra in the region that overlaps with the indium $5^2P_{1/2} \rightarrow 6^2S_{1/2}$ spectrum, the tellurium spectrum was extended by shifting the wavelength of the laser scan by temperature tuning of the diode laser, thus allowing four overlapping regions of the spectrum (each of which was at least 55 GHz wide) to be recorded covering an overall spectral range of 170 GHz. In principle, this region could have been further extended by performing coarse tuning of the grating angle, for example, through the use of a stepper motor.

In a second experiment, a proportional-integral (PI) control algorithm was used to achieve active stabilisation of the laser wavelength by locking it to one of the strong lines in the spectrum of $^{130}Te_2$. This was done using software written by the authors in the LabVIEW environment. The laser-locking was done in the following way: a single-mode scan of the laser wavelength was performed as described above, while viewing on an oscilloscope the measured intensity of the light transmitted through the heated $^{130}Te_2$ vapour cell. The spectral range of this scan was then narrowed down around the line of interest by reducing the amplitude (and dc offset) of the triangular waveforms used to modulate the grating position and the diode laser injection current. Then the modulation was turned off and the PI control program (time constant = 100 ms) was activated. Its purpose was to record the intensity of the laser beam transmitted through the $^{130}Te_2$ cell and thereby to determine a control signal to add to the voltage on the piezo-actuators in the grating mount, thus adjusting the laser wavelength so as to return the value of transmitted intensity to the specified set-point.

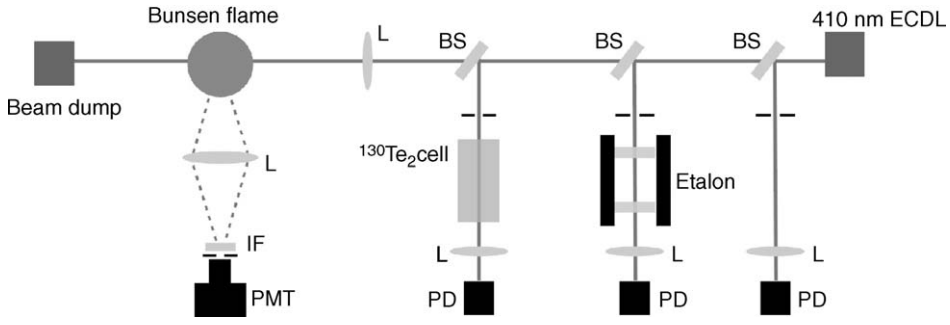

Fig. 1. The experimental set-up for the simultaneous acquisition of $^{130}Te_2$ absorption spectra, and In fluorescence spectra (L: lens; IF: interference filter centred around 451 nm; PMT: photomultiplier tube; PD: photodiode; BS: beam splitter; ECDL: extended cavity diode laser).

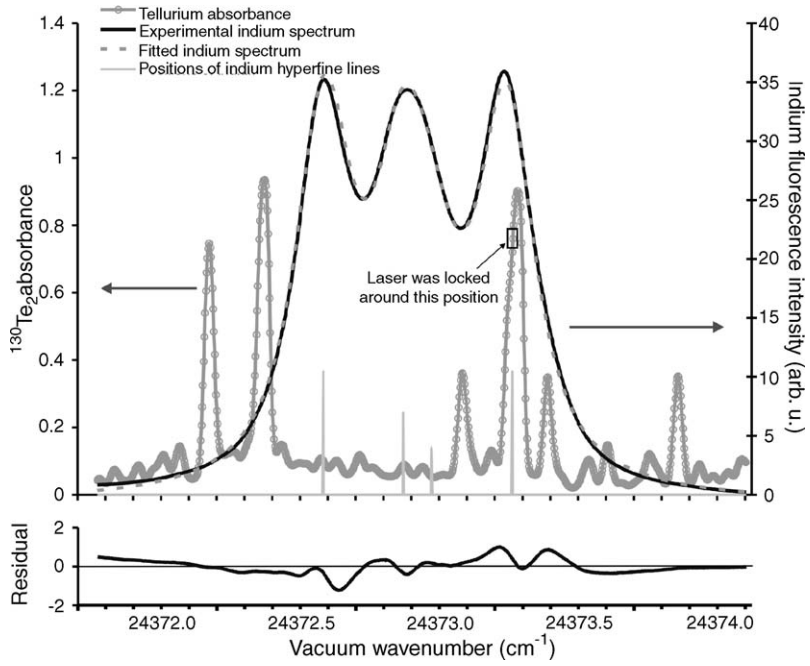

Fig. 2. Spectra of simultaneously acquired $^{130}Te_2$ absorbance and In fluorescence. The spectra correspond to the average of 100 ECDL wavelength scans. Also shown are a theoretical fit of the sum of four Voigt profiles to the indium spectrum, and the locations of the indium hyperfine lines. The residual between the fitted and experimental indium fluorescence spectra is shown on a separate axis.

3. Results and discussion

Fig. 2 shows simultaneously acquired spectra of $^{130}Te_2$ absorbance and atomic indium fluorescence (normalised by the simultaneously recorded laser output power). The spectra were obtained by taking the average of 100 individual single-mode wavelength scans. The scale shown is in vacuum wavenumbers; a correction was made for the pressure shift of the indium spectrum, which was estimated to be around $-0.065\,cm^{-1}$, using the parameter for broadening of In by N_2 [20]. A theoretical fit of the sum of four Voigt profiles was made to the indium fluorescence spectrum in the same way as has been described previously [6], and is also shown in Fig. 2. The good agreement between the experimental data and the fitted spectrum confirms that the laser was emitting on a single-mode throughout the scan. Since the absolute wavelengths of the four hyperfine components of the indium spectrum are known [21], this allowed the absolute frequency scale of the scan to be established.

The composite spectrum shown in Fig. 3 was obtained from the averaged $^{130}Te_2$ absorption spectra that were recorded for four overlapping wavelength ranges. At the positions where the recorded spectra overlapped, the average absorbance is shown. There is a small degree of uncertainty in the absolute values of the absorbance because a slight etalon effect in the cell windows caused a weak ripple on the base line. Nonetheless, the line positions were of principal interest in this work. The dominant source of error in the line positions resulted from the estimation of the FSR of the etalon, which was done using the spacing between the fitted Voigt profiles shown in Fig. 2. The error arises from a combination of the uncertainty in the literature values for the positions of the hyperfine lines [21], and the discrepancy between the results of the fitting process for different experimental spectra. Other sources of error include the estimation of the positions of the hyperfine lines, and the evaluation of the pressure shift for indium. Taken together, these result in an upper estimate of $\pm 0.1\,cm^{-1}$ for the $^{130}Te_2$ line positions shown on Fig. 3 and in Table 1.

The features at $24369.87\,cm^{-1}$, $24372.37\,cm^{-1}$ and $24373.28\,cm^{-1}$, have been identified as being, respectively, the $X0_g^+ \rightarrow B0_u^+(15,0)R(96)$, $X0_g^+ \rightarrow B0_u^+(15,0)P(88)$ and $X0_g^+ \rightarrow B0_u^+(15,0)R(94)$ lines, since they agree to within the error margin with the line positions listed by Jha et al. [22], as shown in Table 1. The other lines observed here do not appear to correspond to any data that have been published in tabular form. In order to assign these, a simple calculation was made, based on published spectroscopic data [11], to predict the positions of

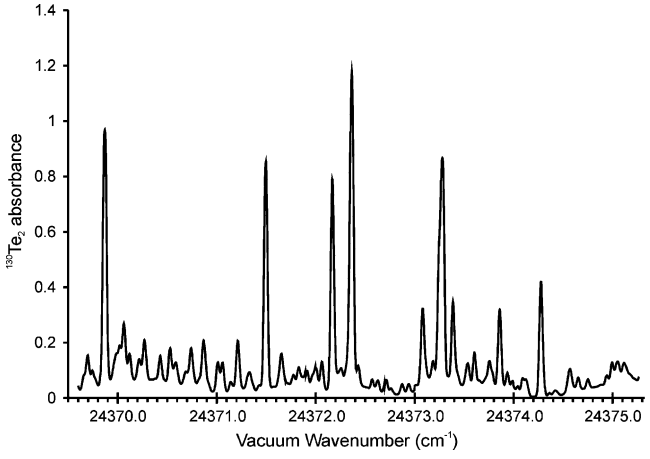

Fig. 3. A composite spectrum of $^{130}Te_2$ absorbance compiled by making ECDL scans over four overlapping wavelength ranges.

Table 1
The wavelengths of the $^{130}Te_2$ lines estimated from the experimental data, and selected line positions from the literature and from calculations based on spectroscopic data

Experimental line positions (cm^{-1})	Identified transitions	Positions listed by Jha et al. [22]	Calculation based on spectroscopic data [11]
24369.87	(15,0)R(96)	24369.93	24370.28
24371.50	(17,1)P(104)		24370.82
24372.17	(17,1)R(110)		24371.54
24372.37	(15,0)P(88)	24372.44	24372.62
24373.08	(16,0)R(148)		24373.47
24373.28	(15,0)R(94)	24373.36	24373.67
24373.39			
24373.86			
24374.28	(16,0)R(154)		24374.75

All of the transitions listed are in the $X0_g^+ \rightarrow B0_u^+$ band. The maximum uncertainty in the experimental line positions has been estimated as $\pm 0.1\ cm^{-1}$.

the lines in a number of bands of the $X0_g^+ \rightarrow B0_u^+$ transition that are situated in this spectral region. The term values for the upper vibrational states are given by Barrow and du Parcq [11] in tabular form and the same authors give an equation to calculate the term values for the lower vibrational state. The rotational constants of the upper and lower electronic-vibrational states are also tabulated [11]. These coefficients were used to calculate the line-positions in the P- and R-branches, and selected results are shown in Table 1. Note that in Te_2 absorption only occurs from lower states having an even value for J'' [23]. The results of the calculation are of limited accuracy since they are derived from parameters that were regressed to experimental data [11] over a wide spectral range. Nevertheless, there is moderate agreement with the experimental data for the X→B (15,0) lines identified above. The calculated line positions also indicate that two of the weaker lines shown in Fig. 3, at 24373.08 cm^{-1} and 24374.28 cm^{-1}, are likely to be $X0_g^+ \rightarrow B0_u^+(16, 0)P(148)$ and $X0_g^+ \rightarrow B0_u^+(16, 0)R(154)$. A further two strong lines in the spectrum, at 24371.50 cm^{-1} and 24372.17 cm^{-1}, are likely to be the P(104) and R(110) lines of the $X0_g{}^+ \rightarrow B0_u{}^+(17,1)$ band. Although there is a discrepancy for this pair between the calculated and experimental line positions, there is a good agreement for the line spacing. This discrepancy is therefore likely to be the result of an inaccuracy in the data used in the calculation, such as in the term value for the $\nu'' = 1$ state or in the rotation constant of one of the levels of the transition. The two lines at 24373.39 cm^{-1} and 24373.86 cm^{-1} in the spectrum shown in Fig. 3 have not being identified; it is probable that these could result from transitions with higher J'' values, or from overlapping weak lines.

The violet ECDL was locked to the $X0_g^+ \rightarrow B0_u^+(15, 0)R(94)$ $^{130}Te_2$ line at a frequency of 24373.3 cm^{-1}, as indicated in Fig. 2. The variations in transmitted intensity of the locked laser were translated into frequency fluctuations using the gradient of the line (change in transmitted intensity per MHz), which was calculated from a spectrum that was recorded immediately prior to the laser-locking experiment. The variation of the laser frequency as a function of time is plotted in Fig. 4; the sampling interval was

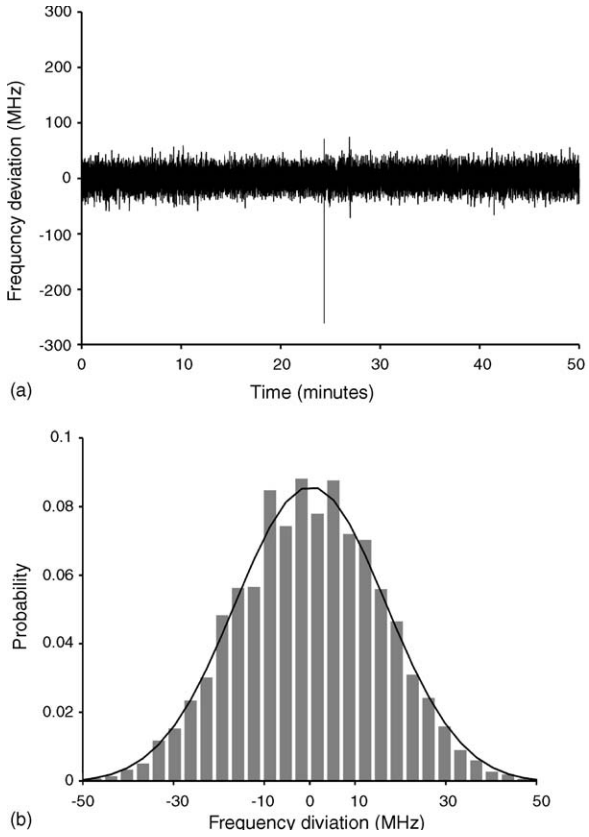

Fig. 4. (a) Variation in frequency of the actively locked 410 nm ECDL; the variation was calculated from the fluctuations in the intensity of the laser beam transmitted through the $^{130}Te_2$ absorption cell. (b) Histogram of deviations from the mean laser frequency.

100 ms. It can be seen that the laser frequency fluctuates around a mean value, rarely deviating by more than 30 MHz; no long-term drift in the laser frequency was observed. One outlying data point is apparent in Fig. 4, and this may be the result of a mechanical disturbance. The control signal increased gradually throughout the experiment, corresponding to a shortening of the extended cavity, to compensate for an apparent increase in the ambient temperature or pressure. In order to stabilise the laser wavelength over longer time periods, it would be necessary to achieve a greater degree of passive stability by improving the temperature stabilisation and pressure isolation of the laser housing [24]. Also shown in Fig. 4 is a histogram of differences from the mean frequency, along with a fitted Gaussian (FWHM = 39.1 MHz). When compared to the typical transition widths at atmospheric pressure, such as that of the $5^2P_{1/2} \rightarrow 6^2S_{1/2}$ transition of atomic indium [6], the fluctuations in the intensity of the locked laser are very small. This set-up is therefore shown to be appropriate to use for frequency stabilisation of diode lasers for use in gas sensing applications at atmospheric pressure.

One particular application in which the techniques described here could be applied would be in two-line atomic fluorescence measurements of flame temperatures [9], which were performed using ECDLs at 410 nm and 451 nm to probe the ratio between the populations in the $5^2P_{1/2}$ and $5^2P_{3/2}$ states of indium atoms seeded to the flame. It would be desirable to extend the appli-

cability of this thermometry technique to dynamic combustion devices. It may be difficult to perform single-mode laser tuning at sufficiently high scan-rates to freeze the turbulent fluctuations in such environments. Instead an approach involving locking the wavelengths of the two lasers and switching rapidly between them using a mechanical chopper or an acousto-optic modulator has been conceived. The results of the experiments described here demonstrate that $^{130}Te_2$ would provide suitable reference lines for such an application.

4. Conclusion

We have shown that the strong $^{130}Te_2$ absorption lines at wavelengths around 410 nm are suitable for use in frequency referencing of laser scans and for active locking of lasers emitting in the violet wavelength region. It is interesting to note that this spectral region is below the range covered by the tellurium atlas [12], which stops at 417 nm. It has been noted that a number of atomic and molecular species have strong electronic transitions in the wavelength range 394–417 nm, and frequency referencing and laser-locking techniques based on $^{130}Te_2$ absorption could therefore find application in gas sensing experiments in this spectral range.

Acknowledgements

This work was sponsored by a grant from the Paul Instrument Fund of the Royal Society. I.S. Burns was in receipt of an EPSRC Cooperative Award in Science and Engineering (CASE), which was partially funded by Rolls-Royce plc. J. Hult was supported by a Research Fellowship from Magdalene College, Cambridge.

References

[1] U. Gustafsson, J. Alnis, S. Svanberg, Am. J. Phys. 68 (2000) 660–664.
[2] H. Leinen, D. Gläßner, H. Metcalf, R. Wynands, D. Haubrich, D. Meschede, Appl. Phys. B 70 (2000) 567–571.
[3] H. Scheibner, St. Franke, S. Solyman, J.F. Behnke, C. Wilke, A. Dinklage, Rev. Sci. Instrum. 73 (2002) 378–382.
[4] O.M. Marago, B. Fazio, P.G. Gucciardi, E. Arimondo, Appl. Phys. B 77 (2003) 809–815.
[5] M.I. Mazurenka, B.L. Fawcett, J.M.F. Elks, D.E. Shallcross, A.J. Orr-Ewing, Chem. Phys. Lett. 367 (2003) 1–9.
[6] J. Hult, I.S. Burns, C.F. Kaminski, Opt. Lett. 29 (2004) 827–829.
[7] K. Hayasaka, Opt. Commun. 206 (2002) 401–409.
[8] C.Y. Park, T.H. Yoon, Jpn. J. Appl. Phys. 42 (2003) L754–L756.
[9] J. Hult, I.S. Burns, C.F. Kaminski, Proc. Comb. Inst. 30 (2005) 1535–1543.
[10] S. Gerstenkorn, P. Luc, Atlas du spectre d'Absorption de la Molecule d'Iode, CNRS, Paris, 1978.
[11] R.F. Barrow, R.P. du Parcq, Proc. R. Soc. A 327 (1972) 279–287.
[12] J. Cariou, P. Luc, Atlas du spectre d'Absorption de la Molecule de Tellure, CNRS, Paris, 1980.
[13] C.F. Kaminski, I.G. Hughes, P. Ewart, J. Chem. Phys. 106 (1997) 5324–5332.
[14] P. Cacciani, W. Hogervorst, W. Ubachs, J. Chem. Phys. 102 (1995) 8308–8320.
[15] M. Hori, R.S. Hayano, E. Widmann, H.A. Torii, Opt. Lett. 28 (2003) 2479–2481.
[16] C. Raab, J. Bolle, H. Oberst, J. Eschner, F. Schmidt-Kaler, R. Blatt, Appl. Phys. B 67 (1998) 683–688.
[17] P. Cancio, D. Bermejo, J. Opt. Soc. Am. B 14 (1997) 1305–1311.
[18] C.E. Wieman, L. Hollberg, Rev. Sci. Instrum. 62 (1991) 1–20.
[19] J. Hult, I.S. Burns, C.F. Kaminski, Appl. Opt. 44 (2005) 3675–3685.
[20] J. Eberz, G. Huber, T. Kühl, G. Ulm, J. Phys. B: At. Mol. Phys. 17 (1984) 3075–3082.
[21] G.V. Deverall, K.W. Meissner, G.J. Zissis, Phys. Rev. 91 (1953) 297–299.
[22] B.L. Jha, K.V. Subbaram, D. Ramachandra Rao, J. Mol. Spectrosc. 32 (1969) 383–397.
[23] R.P. du Parcq, R.F. Barrow, Chem. Commun. (1966) 270a.
[24] H. Talvitie, A. Pietiläinen, H. Ludvigsen, E. Ikonen, Rev. Sci. Instrum. 68 (1997) 1–7.